Supplementary Information

Tunable intrinsic magnetism in 2D Mo_2B_2 via double-transition-metal engineering under electric field and hole doping

Fangrong Zhong [a], Honghai Zhang [a], Dongni Wu [a], Yangfang Liao [a], Jing Xie[a, *1]

[a] *College of Physics and Electronic Science, Guizhou Normal University, Guiyang 550001, China*

1. The ab initio molecular dynamics (AIMD) simulations of $MMoB_2$ (M = V, Cr, Mn, Fe, Co, Ni) monolayers

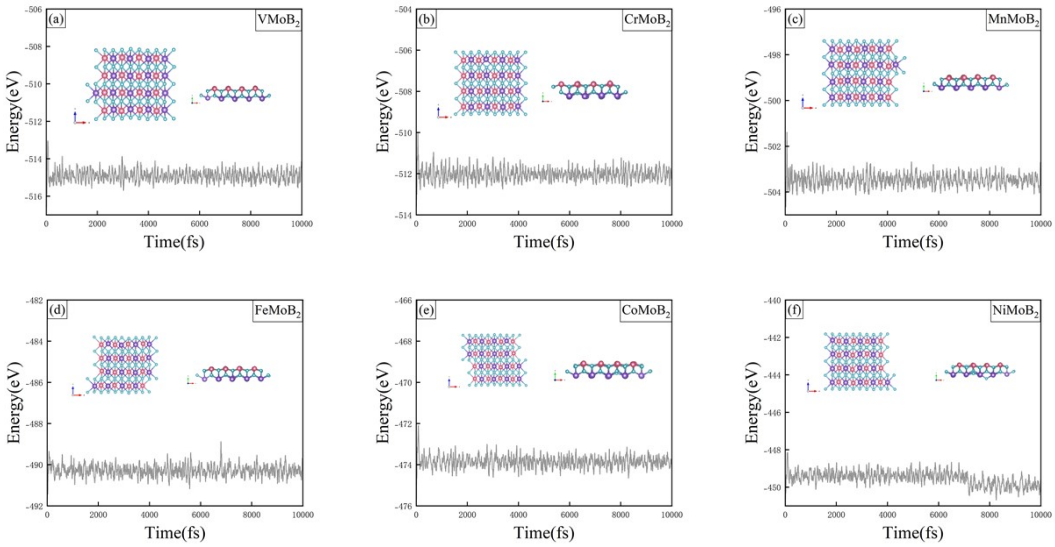

Fig. S1. Energy variation of $MMoB_2$ (M = V, Cr, Mn, Fe, Co, Ni) monolayers at 300 K as a function of time during 10,000 fs ab initio molecular dynamics (AIMD) simulation.

* Corresponding author.
E-mail address: 511492231@qq.com (Jing Xie).

2. The phonon dispersion of $MMoB_2$ (M = V, Cr, Mn, Fe, Co, Ni) monolayers

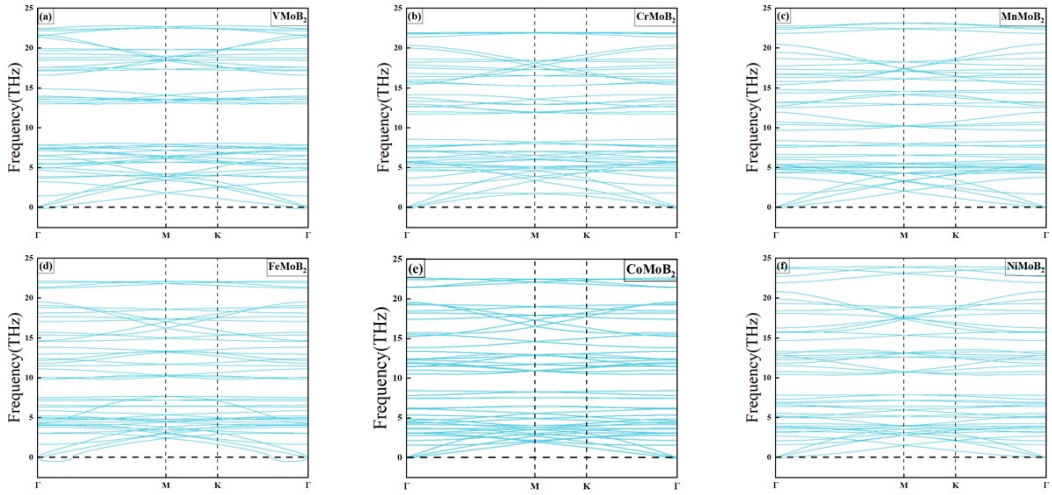

Fig, S2. Phonon dispersion of $MMoB_2$ (M = V, Cr, Mn, Fe, Co, Ni) monolayers.

3. The density of states (DOS) of $MMoB_2$ (M = V, Cr, Mn, Fe, Co, and Ni) monolayers

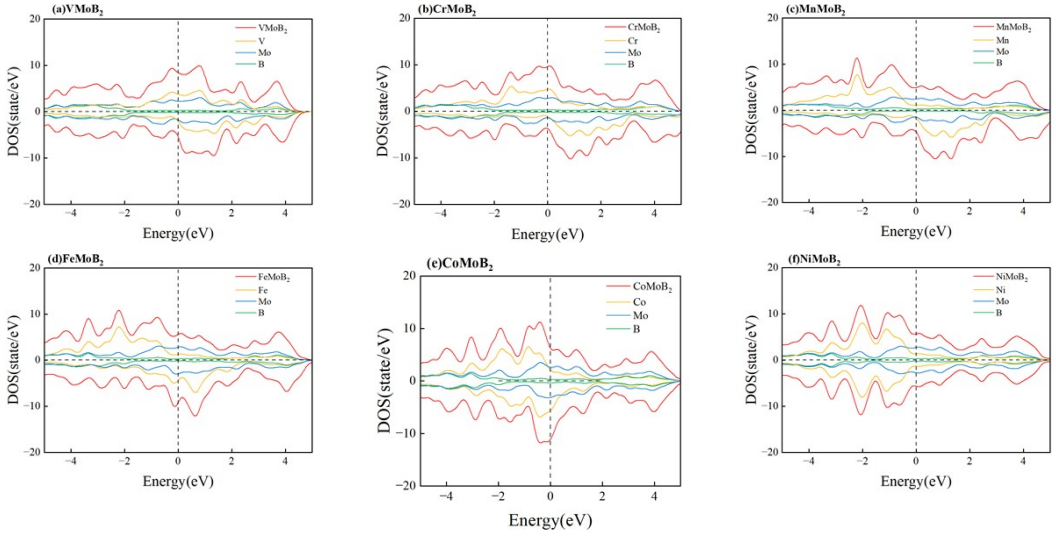

Fig. S3. (a)-(f) The density of states (DOS) of $MMoB_2$ (M = V, Cr, Mn, Fe, Co, and Ni) monolayers.

4. The band centers of the *d*-orbitals for the M atoms in $MMoB_2$ (M = V, Cr, Mn, Fe, Co, Ni) monolayers

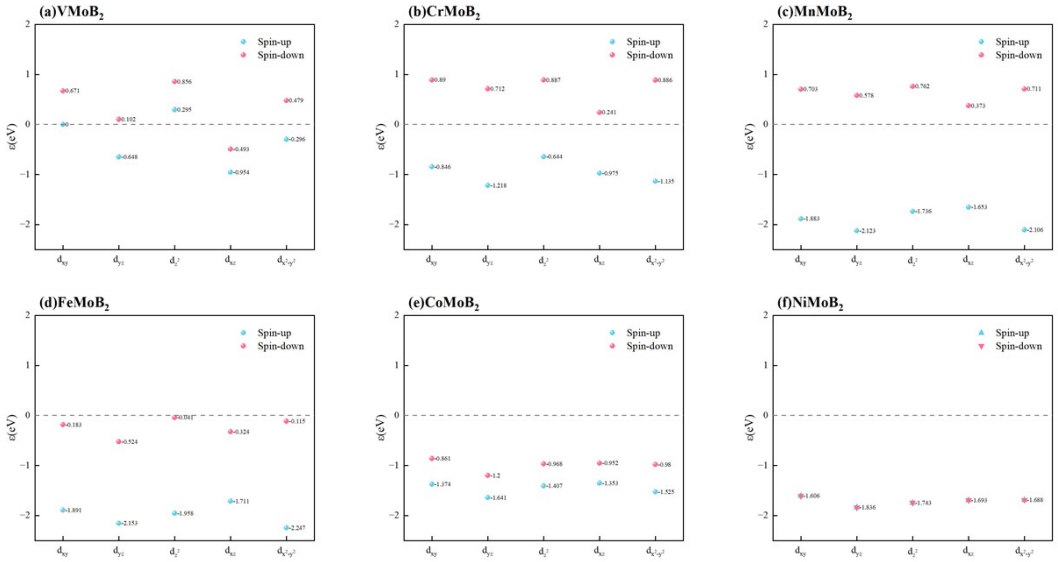

Fig. S4. (a)-(f) Band centers of the *d*-orbitals for the M atoms in $MMoB_2$ (M = V, Cr, Mn, Fe, Co, Ni) monolayers.

5. The evolution of the magnetic ground state in $MMoB_2$ (M = V, Cr, Mn, Fe, Co) monolayers under the application of a vertical electric field and hole doping

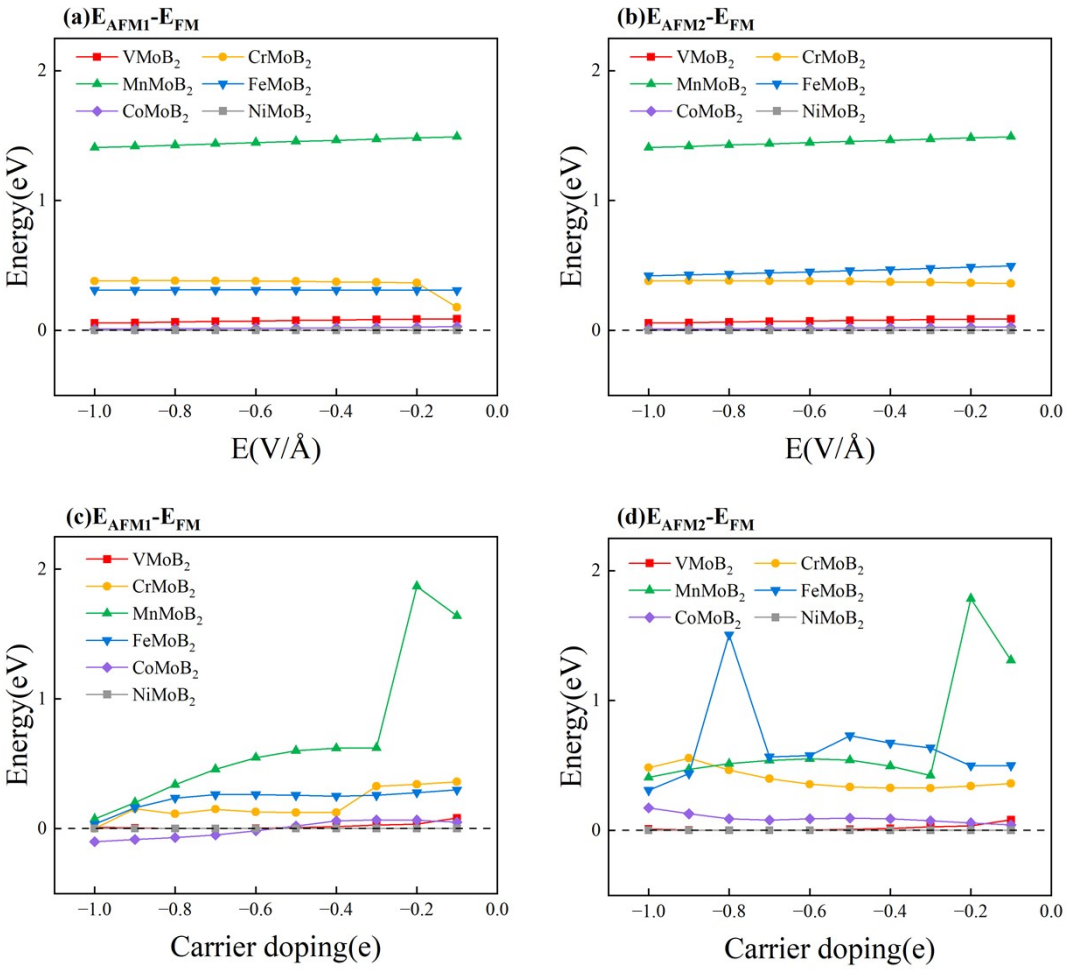

Fig. S5. Evolution of the magnetic ground state in $MMoB_2$ (M = V, Cr, Mn, Fe, Co) monolayers under the application of a vertical electric field and hole doping.

6. The total magnetic moment and magnetic moment on the M atom in $MMoB_2$ (M = V, Cr, Mn, Fe, Co) monolayers as a function of applied electric field strength

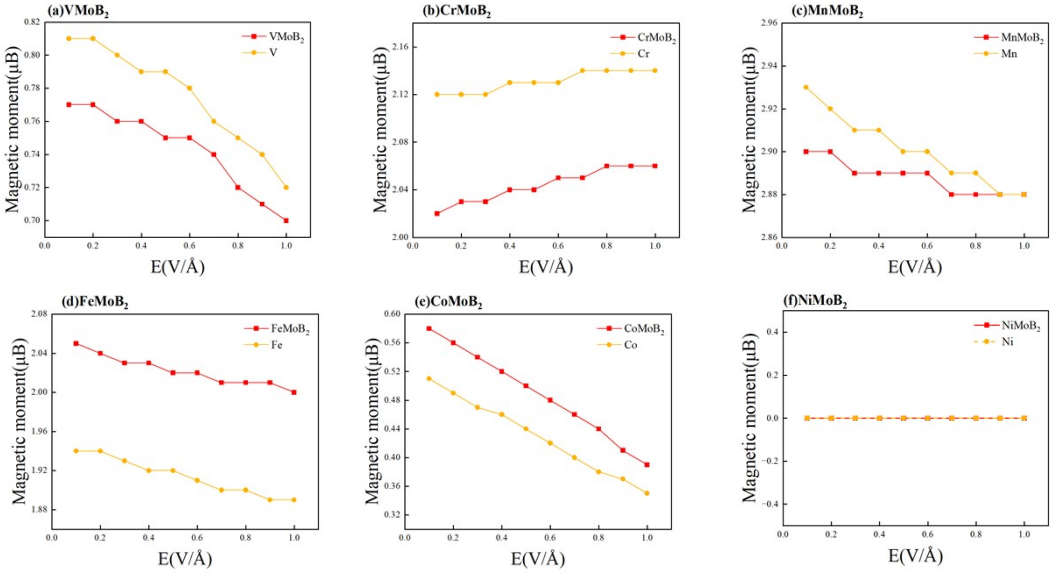

Fig. S6. Total magnetic moment and magnetic moment on the M atom in $MMoB_2$ (M = V, Cr, Mn, Fe, Co) monolayers as a function of applied electric field strength.

7. The electronic band structures of $MMoB_2$ (M = V, Cr, Mn, Fe, Co) monolayers under different electric field strengths

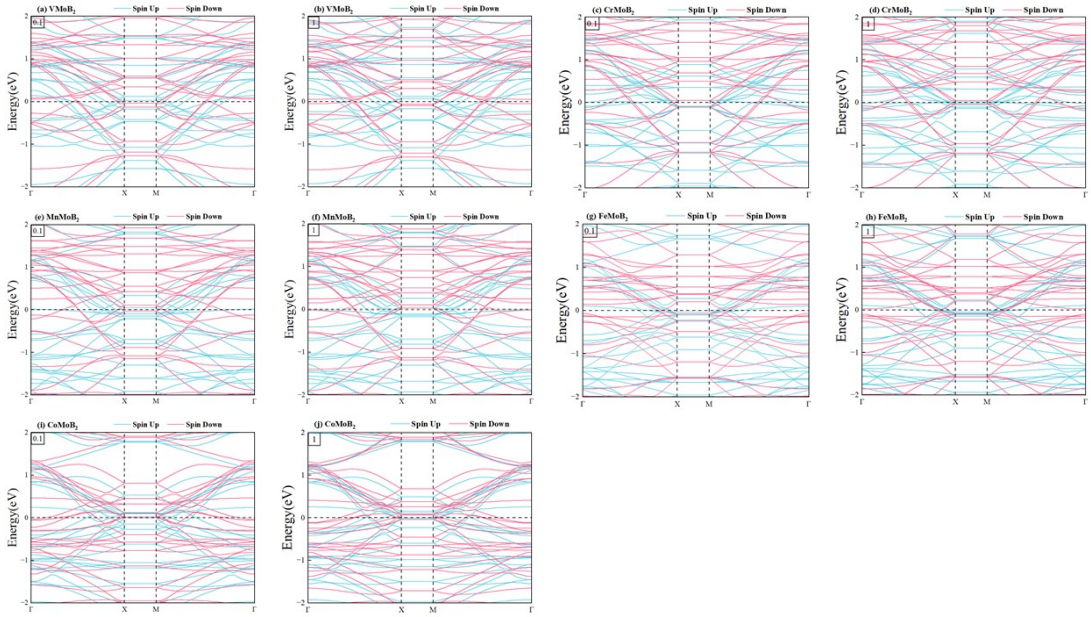

Fig. S7. (a)-(j) Electronic band structures of $MMoB_2$ (M = V, Cr, Mn, Fe, Co) monolayers under different electric field strengths.

8. The PDOS of the M atom d-orbitals in $MMoB_2$ (M = V, Cr, Mn, Fe, Co) monolayers under electric field strengths of 0.1 V/Å and 1.0 V/Å

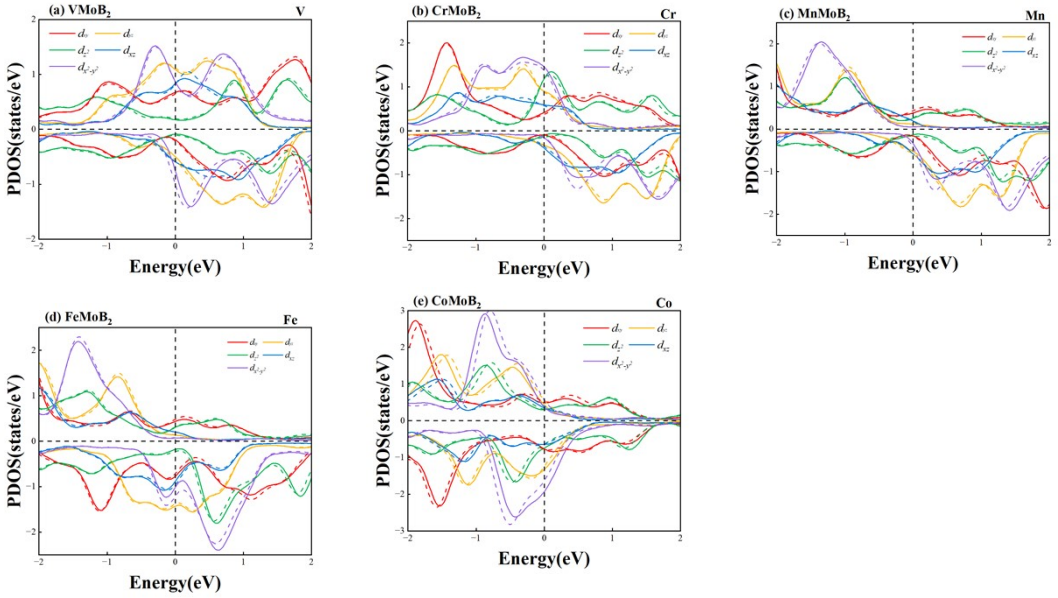

Fig. S8. (a)-(e) PDOS of the M atom d-orbitals in $MMoB_2$ (M = V, Cr, Mn, Fe, Co) monolayers. The solid and dashed lines represent the PDOS under electric field strengths of 0.1 V/Å and 1.0 V/Å, respectively.

9. The orbital-resolved MAE of the *d*-orbitals for the Mo, Cr, Mo, and Fe atoms in $MMoB_2$ (M = V, Cr, Mn, Fe, respectively) monolayers under an electric field strength of 0.1 V/Å

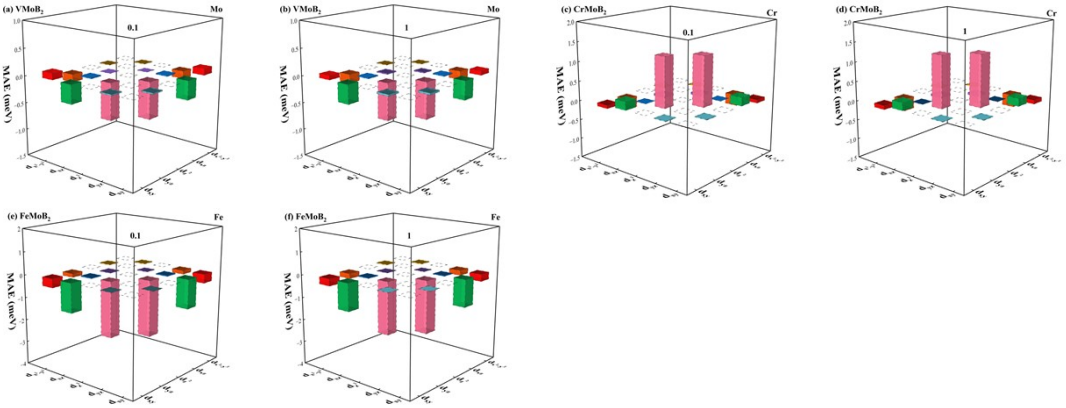

Fig. S9. Orbital-resolved MAE of the *d*-orbitals for the Mo, Cr, Mo, and Fe atoms in $MMoB_2$ (M = V, Cr, Mn, Fe, respectively) monolayers under an electric field strength of 0.1 V/Å.

10. The total magnetic moment and magnetic moment on the M atom in $MMoB_2$ (M = V, Cr, Mn, Fe, Co) monolayers as a function of hole doping concentration

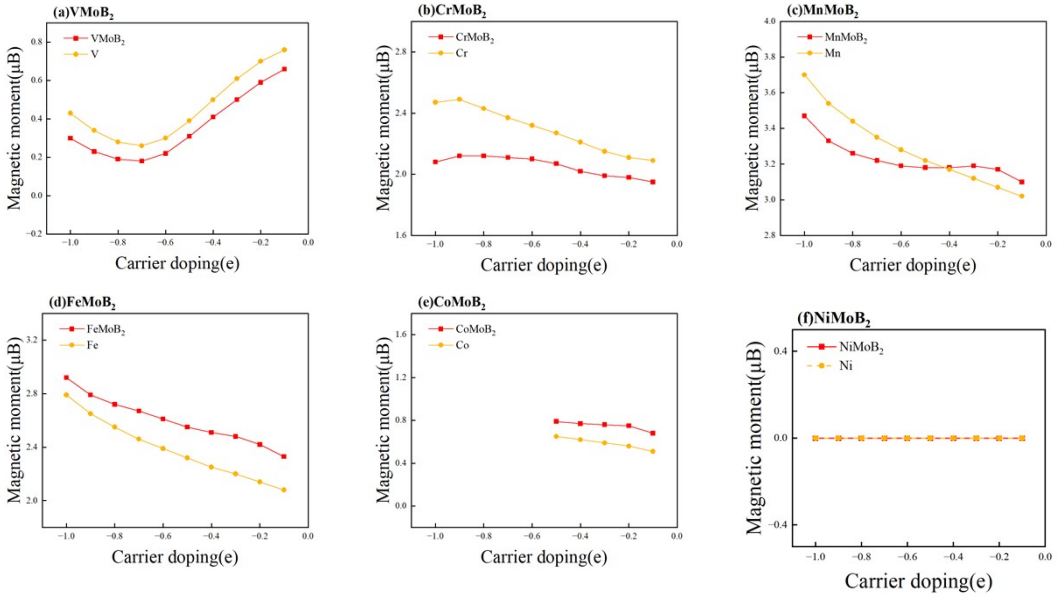

Fig. S10. Total magnetic moment and magnetic moment on the M atom in $MMoB_2$ (M = V, Cr, Mn, Fe, Co) monolayers as a function of hole doping concentration.

11. The electronic band structures of MMoB2 (M = V, Cr, Mn, Fe, Co) monolayers at different hole doping concentrations

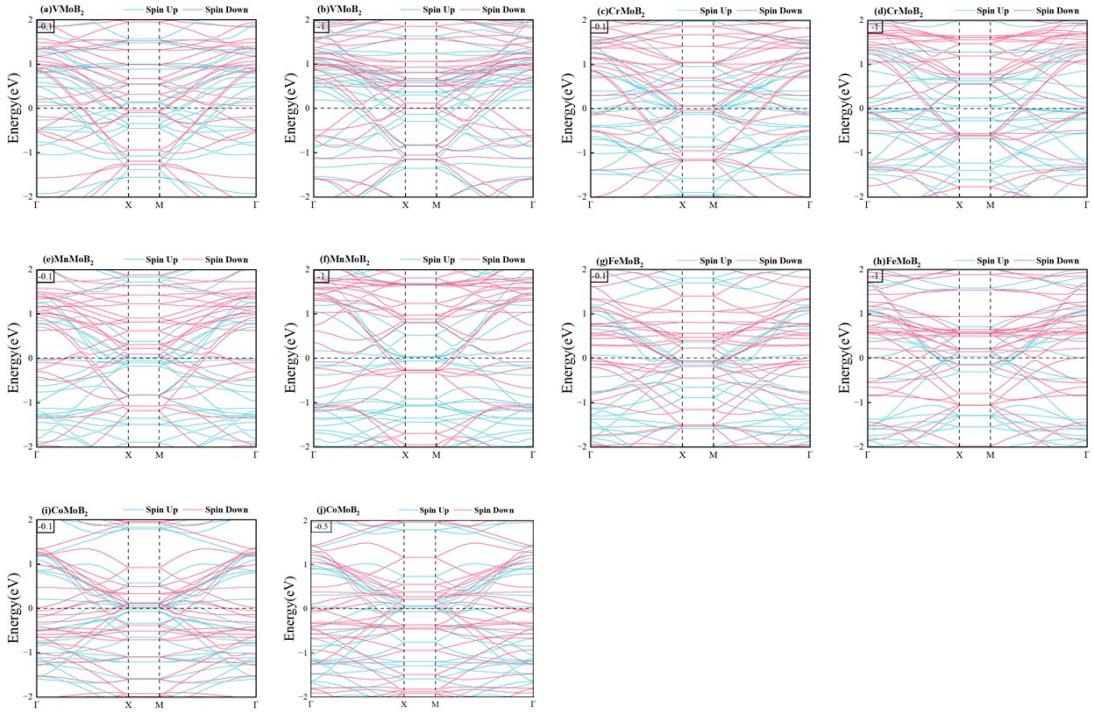

Fig. S11 (a)-(j) Electronic band structures of $MMoB_2$ (M = V, Cr, Mn, Fe, Co) monolayers at different hole doping concentrations.

12. The PDOS of the M atom *d*-orbitals in $MMoB_2$ (M = V, Cr, Mn, Fe, Co) monolayers at hole doping concentrations of -0.1 e and -1.0 e

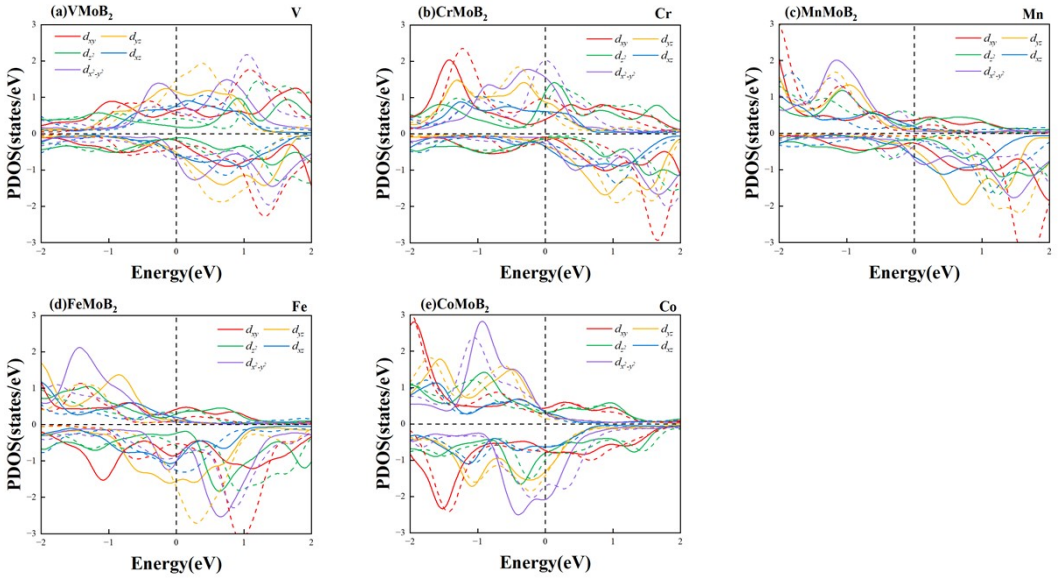

Fig. S12. (a)-(j) PDOS of the M atom *d*-orbitals in $MMoB_2$ (M = V, Cr, Mn, Fe, Co) monolayers. The solid and dashed lines represent the PDOS at hole doping concentrations of -0.1 e and -1.0 e, respectively, except for Co (dashed line at -0.5 e).

13. Band centers of the Fe atom d-orbitals at hole doping concentrations of -0.1 e and -1.0 e, respectively

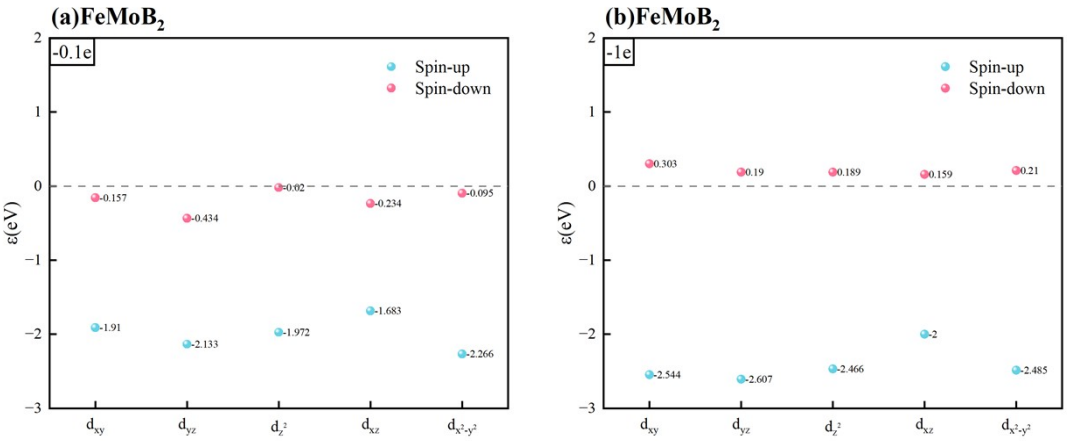

Fig. S13. Band centers of the Fe atom d-orbitals at hole doping concentrations of -0.1 e and -1.0 e, respectively.

14. The orbital-resolved MAE of the *d*-orbitals for the Mo, Mo, Fe, and Co atoms in $MMoB_2$ (M = V, Mn, Fe, Co, respectively) monolayers at a hole doping concentration of -0.1 e

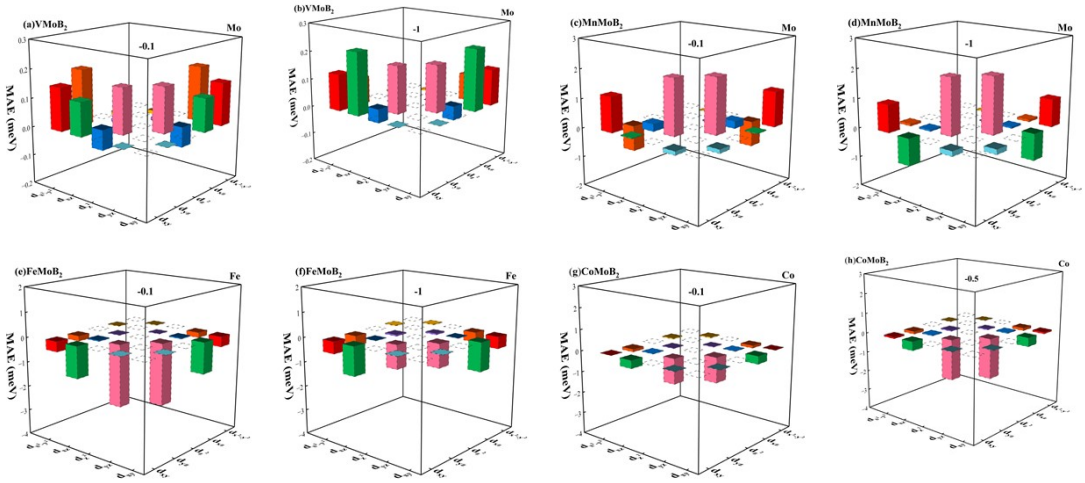

Fig. S14. Orbital-resolved MAE of the d-orbitals for the Mo, Mo, Fe, and Co atoms in $MMoB_2$ (M = V, Mn, Fe, Co, respectively) monolayers at a hole doping concentration of -0.1 e.

15. Magnetic exchange parameters of $MMoB_2$ (M = V, Cr, Mn, Fe, Co) monolayers under different hole doping concentrations

Table S1. Variation of magnetic exchange parameters J_1 (meV) and J_2 (meV) with hole doping concentration from -0.1 e to -1.0 e for $MMoB_2$ monolayers.

	$VMoB_2$		$CrMoB_2$		$MnMoB_2$		$FeMoB_2$		$CoMoB_2$	
	J_1	J_2	J_1	J_2	J_1	J_2	J_1	J_2	J_1	J_2
-0.1	2.59	1.3	5.01	2.5	4.55	3.42	3.91	0.38	1.32	0.9
-0.2	1.12	0.56	4.75	2.38	6.2	3.39	3.9	0.22	1.82	1.14
-0.3	0.86	0.43	4.53	2.26	1.47	1.43	4.97	-0.47	2.31	0.92
-0.4	0.48	0.24	4.53	-0.53	1.72	1.29	5.25	-0.67	2.79	0.43
-0.5	0.23	0.11	4.65	-0.61	1.88	1.15	5.69	-0.84	2.99	-0.86
-0.6	0.07	0.04	4.94	-0.69	1.91	0.95	4.51	-0.2	2.81	-1.95
-0.7	0.01	0.01	5.52	-0.68	1.87	0.65	4.42	-0.16	2.46	-2.77
-0.8	0.03	0.02	6.44	-1.65	1.78	0.28	11.77	-4.04	2.81	-3.58
-0.9	0.12	0.06	7.74	-1.74	1.64	-0.12	3.42	-0.45	4.01	-4.65
-1.0	0.29	0.15	6.71	-3.34	1.41	-0.45	2.42	-0.94	5.44	-5.89